JOURNAL OF MATERIALS SCIENCE **35** (2000) 2847–2854

TEM study of the interface between HIPed silicon nitride and encapsulation borosilicate glass

A.-K. WESTMAN, L.-Y. WEI
Department of Material Science and Production Technology,
Luleå University of Technology, S-971 87 Luleå, Sweden

A transmission electron microscope study has been made of a silicon nitride component with 6 w/o yttrium oxide as a sintering aid hot isostatically pressed (HIP) with an encapsulation glass of borosilicate. The TEM study concentrated on the interface region between ceramic and glass. Two different types of hexagonal boron nitride were formed near the interface. One, with a textured structure, seemed to nucleate heterogeneously on the surfaces of silicon oxynitride grains. The (001) planes of the crystals extended outwards, giving a thickness of approximately 0.5 microns. The other type formed as hexagonally shaped grains separate from the first type and appeared to have grown as several segments in different directions around a nucleus. In each segment BN layers are parallel to each other and perpendicular to their common $[001]_{BM}$ direction. This second type of BN crystal was also detected a little further from the surface within the silicon nitride. The volume fraction of additive glassy phase tended to be lower in this surface region than in the bulk. Possible mechanisms of prevention of encapsulation glass penetration into the porous ceramic component during HIP were discussed. © *2000 Kluwer Academic Publishers*

1. Introduction

Structural ceramics exhibit beneficial properties such as high strength, wear resistance, chemical resistance and ability to sustain high temperatures. It follows that in many applications the surface properties of the component are critical. This is a particularly important consideration when hot isostatic pressing (HIP) is used for densification. HIP has the advantage that it can be used to produce components with complicated shapes but the porous pre-formed body has to be encapsulated in a gas tight envelope for the pressure to act. For ceramics this encapsulation is usually of glass, for example quartz or borosilicate. Since the glass and porous ceramic are normally in direct contact during the sintering process, an influence on the surface properties is probable. Since this densification method has a potential for near net or net shape production, any surface interactions are of considerably significance. In the present study a model system of a silicon nitride and a borosilicate glass has been investigated, with emphasis on the microstructure of the interfacial region between the nitride and the glass, that is the subsequent surface of the ceramic.

The microstructure of HIPed, yttria-doped silicon nitride has been investigated by a number of authors [e.g. 1–3]. The structure contains β-silicon nitride grains with a relatively large amount of glassy phase. Some residual grains of α-silicon nitride with rounded shape as well as silicon oxynitride grains can be found. A secondary crystalline phase frequently detected is α-yttrium disilicate while β-yttrium disilicate is observed occasionally. As far as the present authors are aware, no previous TEM study on the HIPed surface region has been reported.

2. Experimental

The silicon nitride* powder containing 6 w/o yttria† as a sintering aid was formed by cold isostatic pressing (CIP) at a pressure of 300 MPa followed by machining. The samples were cubes with a size of 10 × 10 × 10 mm^3. A borosilicate glass with a composition of 60 w/o B_2O_3 and 40 w/o SiO_2 functioned as encapsulation which was applied by a proprietory technique. The HIP-cycle, employing an argon pressure medium, involved a temperature increase to 1180 °C and a hold time at this temperature of one hour during which the pressure was increased to 130 MPa. After this the temperature was raised at 600 °C/h to a maximum of 1750 °C while the pressure was raised to 160 MPa. The hold time at maximum temperature was one hour. The TEM specimen preparation was based on a technique developed by Barna [4]. Two pieces of the silicon nitride material with the interface towards the encapsulation glass on one side, were mounted in a titanium specimen carrier with a diameter of 3 mm and a thickness of 0.5 mm. The silicon nitride pieces were placed in a central window (1 mm × 1.9 mm) in the carrier, with the nitride/glass interfaces facing each other in the centre. Aluminium strips were used to fill up the gaps around the specimen

---

* Siconide P95, Permascand AB, Sweden.

† 99.9F, Rhone-Poulenc, France.

and thereby fix it before all remaining voids were filled with a glue. The specimens were ground and polished to a thickness of approximately 50 microns. Ion beam etching with argon ions (in a Bal-Tec RES010 unit) was used to obtain an electron beam transparent area. A typically setting was 2.5 mA and 8 kV with one side milling and a milling angle of 5 degrees. A more detailed description of the TEM specimen preparation technique is given in [5]. The microscope used in this study was a JEOL 2000 EX with an acceleration voltage of 200 kV and a LaB_6 filament. The microscope was equipped with a LINK EDS (energy dispersive x-ray spectrometer) system for elemental analysis. Since the window of the EDS-detector was of beryllium, the lowest detectable atom number was 11 (sodium). A specimen holder with graphite container was used for EDS analysis. During diffraction analysis a double-tilt specimen holder was used which permitted tilting of the specimen in two directions.

Three different areas of the specimen were examined namely (i) the bulk, approximately 500 microns from the HIP surface (ii) an area at the nitride/glass interface and (iii) an area approximately 8 microns into the ceramic.

3. Results and discussion

3.1. Microstructure of the bulk

In Fig. 1a is seen a micrograph of the bulk area. The microstructure comprises grains in a size range of approximately 0.1–2 microns. There are larger and smaller grains with faceted shapes which is a typical appearance of β-silicon nitride. Some more rounded grains and smaller grains with a circular cross section can also be seen.

A dark field image formed by diffused scattered electrons is shown in Fig. 1b. The lighter areas are amorphous. (Note the bright grains to the left in the picture which show up due to diffracted beams from these two grains falling into the objective aperture. The tiny bright dots are dust.) The material contains relatively large amount of residual glassy phase. Some regions of this glassy phase contain smaller grains. A thin intergranular amorphous phase is visible between adjacent grains.

The compositions of different grains as well as of the glassy phase were examined by STEM/EDS. In most of the grains only Si was detected. The spectrum for some of the smaller grains also contained a very low Y peak, which could however originate from the surrounding glass. Different compositions were obtained for the glass pockets but all contained Si and Y. Fig. 2a shows the spectra from a large pocket with smaller grains within it. The YL_α-peak height is approximately 1/4 of the adjacent SiK_α-peak. Another glass pocket, containing no small grains, contained more yttrium, Fig. 2b. (The Ti peak originates from the specimen carrier.) A quantitative estimation of the relative amounts based on a few analyses gave the following results. The composition in the pocket with small grains was 20 atomic percent Y/80 atomic percent Si whereas in the pocket without grains the ratio was 50%Y/50%Si.

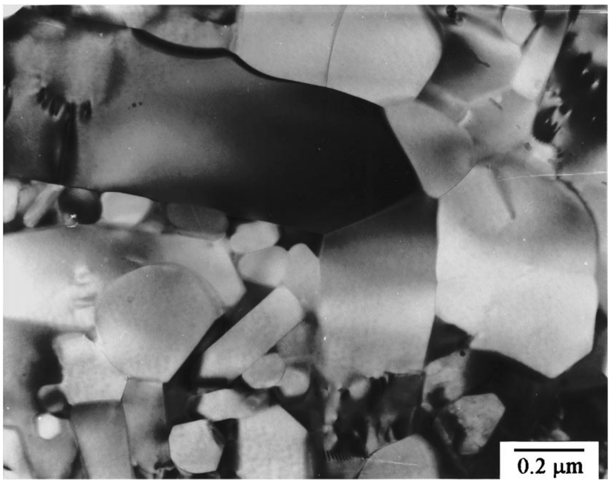

(a)

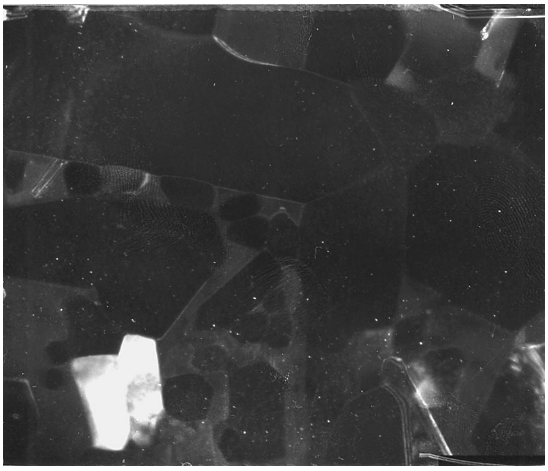

(b)

Figure 1 (a) TEM, microstructure of the bulk; (b) TEM dark field image formed by diffused scattered electrons, the same area as in (a).

Some Fe-containing impurities could also be seen in the microstructure. Fig. 3a shows an impurity grain with a diameter of 0.5 microns and with a small spotty structure. The matrix contains Si, Fe and Ni, as shown in EDS spectrum in Fig. 3b. EDS spectrum of the small dark dots on the impurity grains shows peaks of P, V, Cr, Ni and W in addition to peaks of Si and Fe (Ti peak presumed from the specimen carrier). The dark particles are very tiny, less than 20 nm, therefore the spectrum in Fig. 3c probably is a result of two overlapped phases. The composition indicates that the impurity could be stainless steel. Possibly originating from the raw material powder or from processing of the green body.

3.2. Microstructure in the surface region

A micrograph of the specimen surface is seen in Fig. 4, with the adjacent glue at the top of the picture. Close to the glue is a region, here approximately 1 micron in thickness, which first was taken to be the amorphous encapsulation glass. However, some structure could be detected and with appropriate tilting a layered structure with random orientations appeared. This turned out to be hexagonal boron nitride, BN, deduced from extensive electron diffraction. The thickness of the layer varied along the surface. In places it was almost absent.

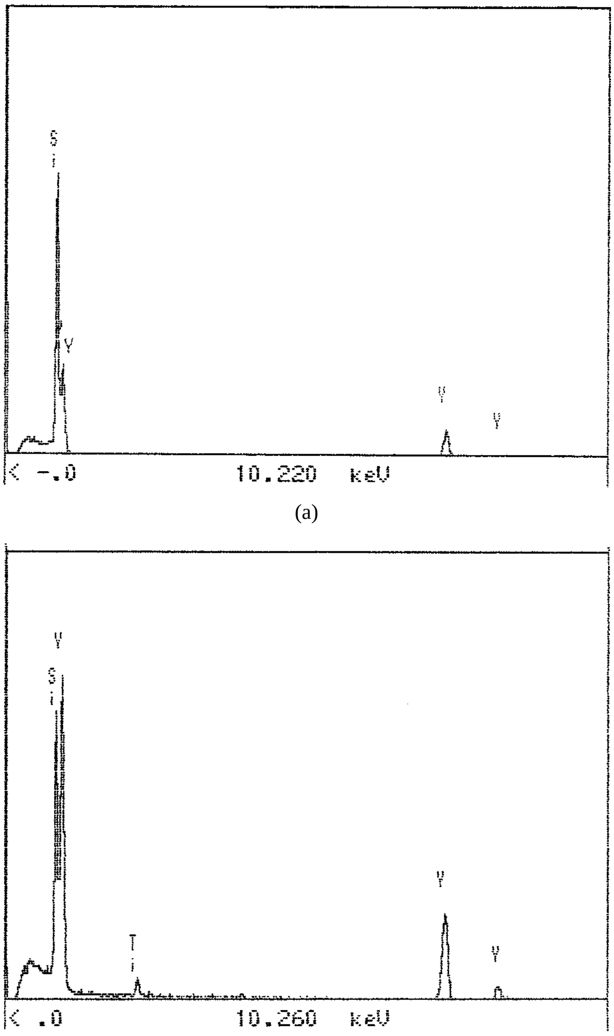

(a)

(b)

Figure 2 EDS spectrum of two different glass pockets; (a) with grains and (b) without grains.

Pure encapsulation glass could not be detected although it was present on the surface of the original specimen. Beneath the outer BN layer a more textured BN structure is seen adjacent to silicon oxynitride grains with silicon nitride grains further in. (Shown in detail in Figs 5–7.)

Fig. 5a shows the boron nitride with two different appearance. BN formed on the surface of a ceramic grain had a more textured structure. Further out, to the right in the picture, the other type of BN, with a more random orientation of the layered structure, is seen.

A selected area electron diffraction (SAED) from the textured area is seen in Fig. 5b, while a SAED from the larger area with both types of grains is shown in Fig. 5c. The rings in the latter diffraction pattern are due to the presence of many orientations of BN crystal platelets relative to the direction of the electron beam. Table I gives a comparison between the interplanar spacings of a hexagonal BN lattice ($a = 2.504$ Å, $c = 6.661$ Å) and the spacings calculated from the diffraction rings shown in Fig. 5c.

The agreement of the two sets of values indicates that the phases with the layer structure are hexagonal BN crystals. (Some possible diffractions are absent due to orientation of the crystals.)

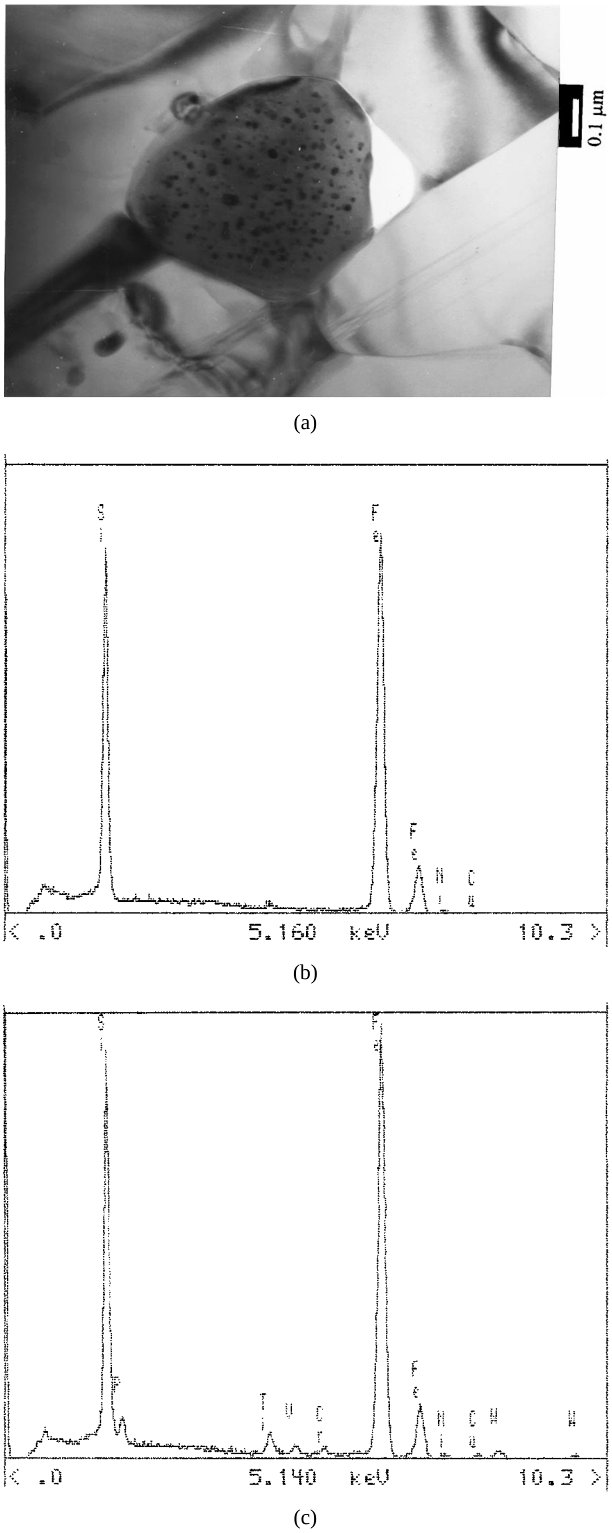

(a)

(b)

(c)

Figure 3 (a) TEM micrograph showing an impurity grain; (b) EDS of matrix; (c) EDS of darker spots; see text.

Marked in Fig. 5a is a glass pocket rich in Si and Y, for which the EDX spectrum is shown in Fig. 5d. The Y/Si atomic ratio is determined to be 34/66.

A bright field image of other textured BN grains formed on the ceramic surface is shown in Fig. 6a, with a SAED pattern in Fig. 6b. The (001) planes are perpendicular to the paper and extend in the direction of the linear structure. It can be seen that the layers vary slightly in orientation within a range of ±15 degrees. Fig. 6c is a dark field image formed by part of one BN

TABLE I Hexagonal BN, d-values and hkl-planes

BN lattice *hkl*	d-values (Å)	Measured from the SAED, Fig. 5c. d-value (Å)
002	3.330	3.321
100	2.169	2.166
101	2.062	
102	1.818	
004	1.664	
103	1.551	
104	1.320	
110	1.252	1.240
112	1.172	1.163
105	1.135	
006	1.110	
200	1.084	1.075

Figure 4 TEM micrograph of the specimen surface.

diffraction arc in the SAED while the dark field image in Fig. 6d is formed by one of the distinct spots. Another crystalline phase with an elongated appearance was present in between the BN layers. EDS-analysis of this phase shows the presence of Y and Si, (atomic ratio 26/74) (see Fig. 6e). Anyhow, d-values from its diffraction pattern fit α-$Y_2Si_2O_7$, but only two different planes of the phase was represented and no unambiguous determination could be obtained. Further work on this crystal phase is needed.

Systematic electron diffraction was carried out on grains adjacent to the textured boron nitride layers in order to identify their crystal structure and silicon oxynitride was detected (Fig. 7a). Diffraction patterns from one Si_2N_2O grain are presented in Fig. 7b and c. In the micrograph the BN appears to nucleate at the surface of the oxynitride grains. In Fig. 5a the same appearance with heterogeneous nucleation of BN at the surface of the adjacent grain seems to have taken place. The BN grains grow by extension of the (001) planes. Every single segment contains several layers parallel to each other.

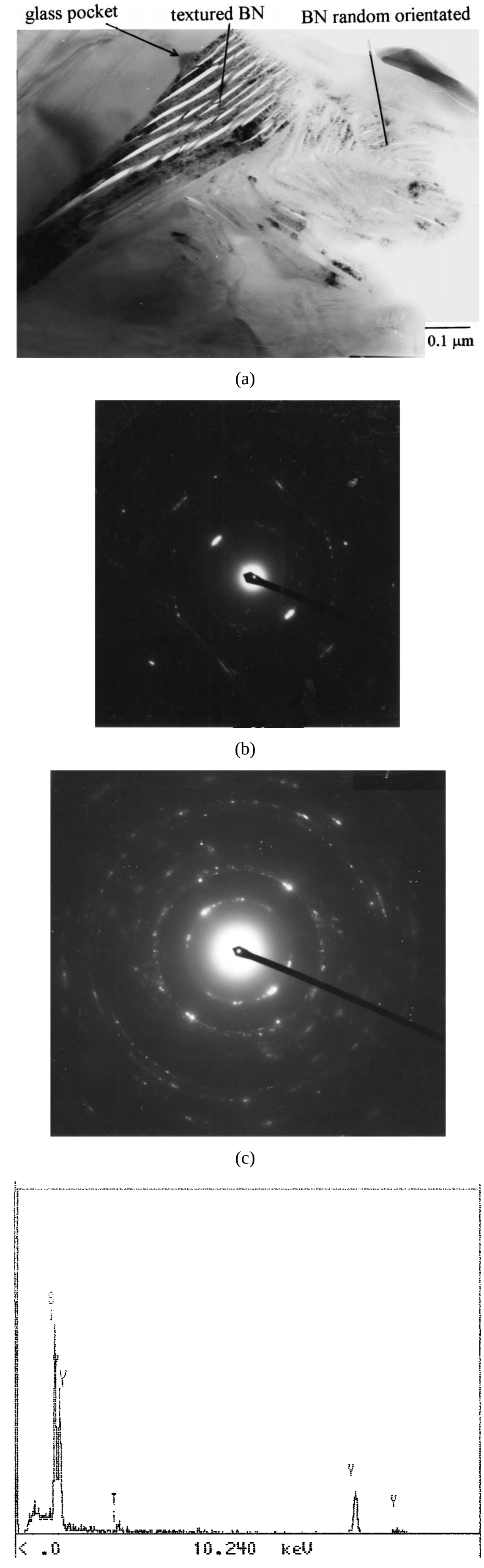

Figure 5 (a) TEM micrograph of two different types of hexagonal BN; (b) SAED from the textured structure in (a); (c) SAED from a larger area in (a); (d) EDS spectrum of glass pocket marked in (a).

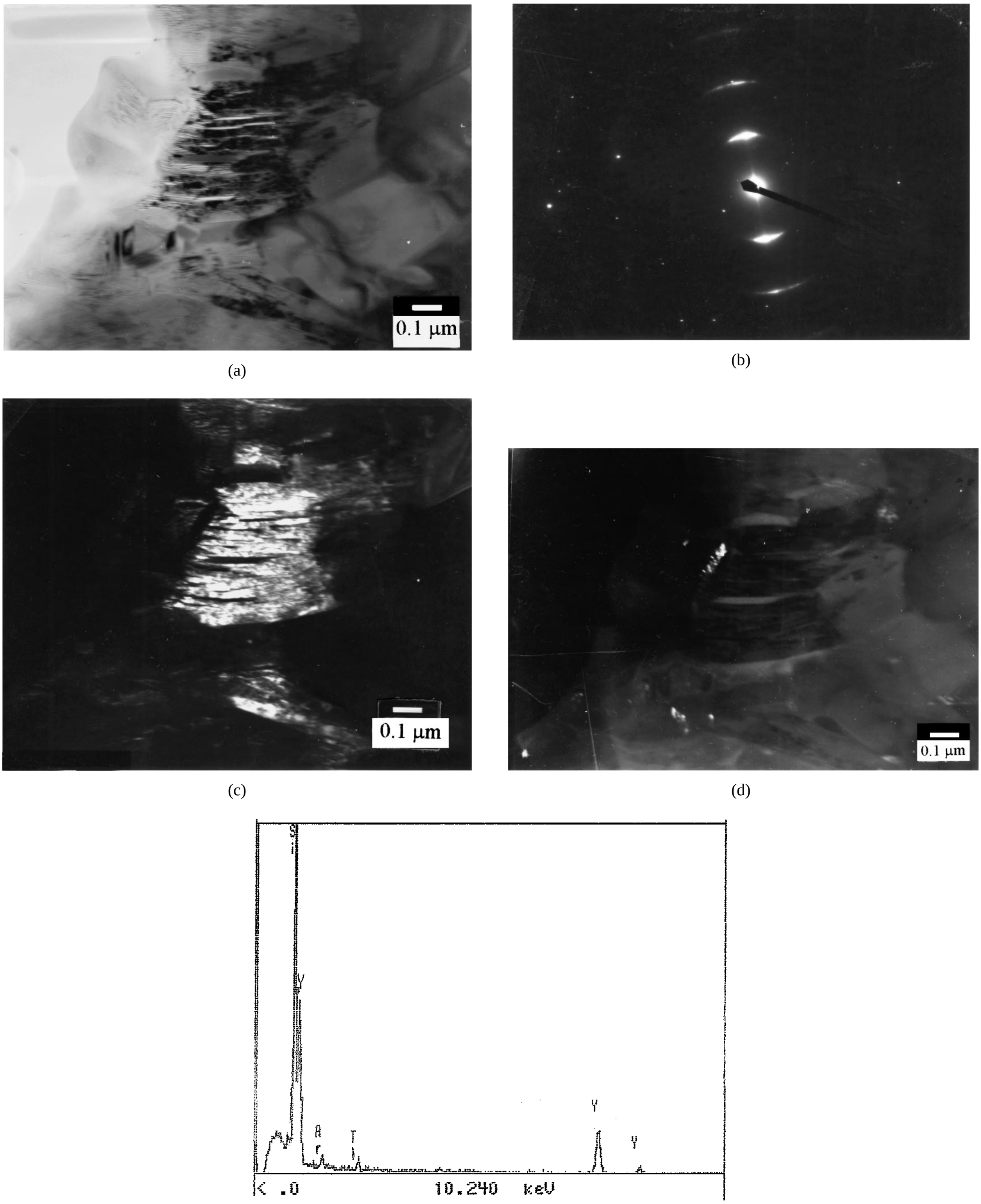

(a) (b) (c) (d) (e)

Figure 6 (a) TEM of layered structure at the surface. Bright field image; (b) SAED, layered structure at the surface, see (a); (c) dark field image formed by part of one BN diffraction arc, in (b); (d) dark field image formed by one of the distinct spots, in (b); (e) EDS of the light area in micrograph (d).

Approximately 8 microns in from the surface, the general appearance of the microstructure is as shown in Fig. 8a. One difference compared to the structure in the bulk is a somewhat lower volume fraction of glassy phase. Fig. 8b is a dark field image formed by diffused scattered electrons taken from the lower-right area in Fig. 8a. The glassy layer between the grains is seen but no large glass pockets are found as in Fig. 1b.

Another difference is the appearance of the same BN structure as was found at the very surface. These were not easy to detect. First a (002) diffraction of the BN phase was found in a diffraction pattern from the central area in Fig. 8a, then a dark field image of BN was obtained by using this $(002)_{BN}$ deflected beam. After tilting a typical appearance of the BN phase showed up. Diffraction rings of BN similar to that in Fig. 5c were

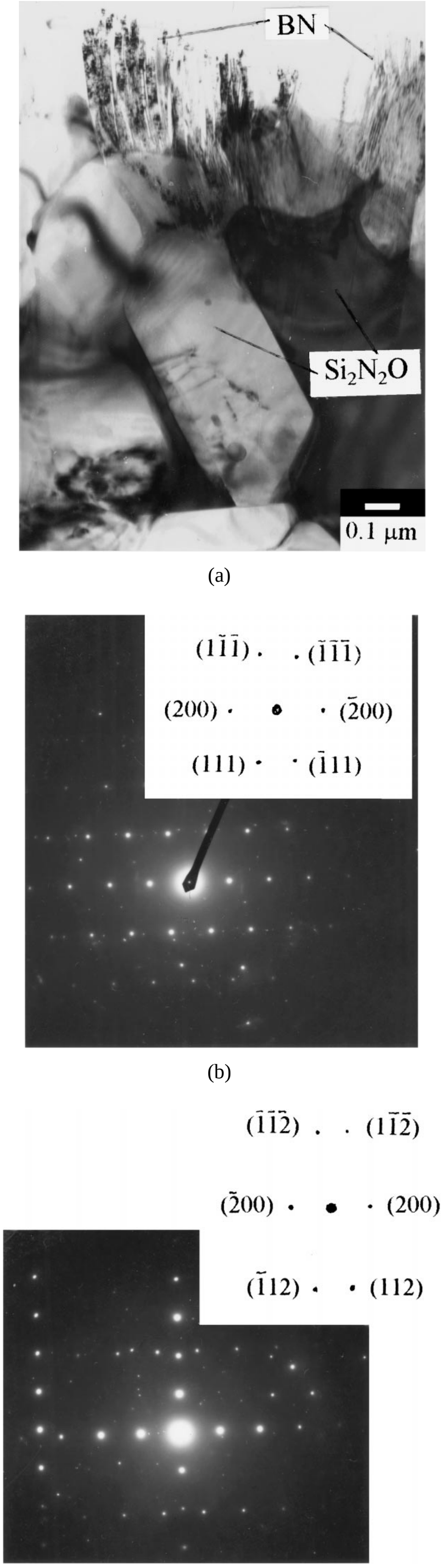

(a)

(b)

(c)

Figure 7 (a) TEM micrograph of the surface area. BN grains seems to have nucleated at the adjacent grain which are silicon oxynitride. SAED of silicon oxynitride with zone axis; (b) [01-1] and (c) [02-1], the angle between the axis is 17.6 degrees.

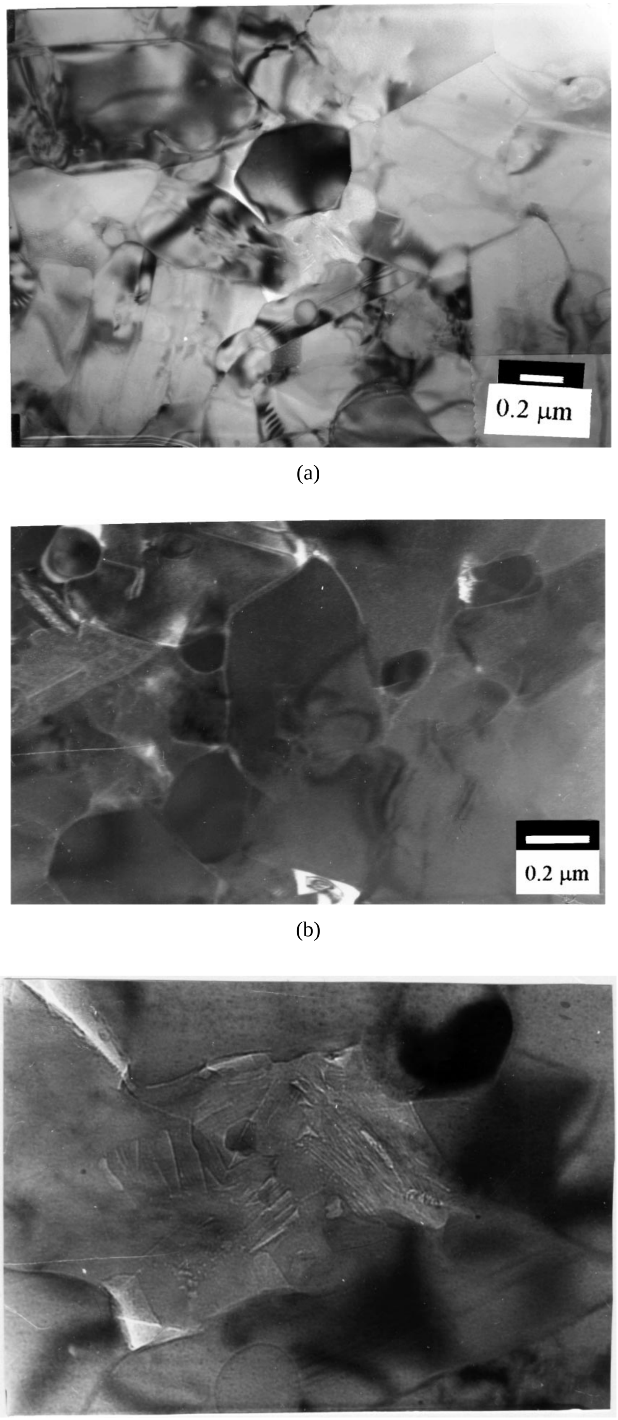

(a)

(b)

(c)

Figure 8 TEM micrograph of area approximately 8 microns from the interface. (a) Shows the general microstructure; (b) give a dark field image produced by diffused scattered electrons; (c) shows the BN structure.

obtained in this orientation. Fig. 8c is an enlarged picture of BN phase which was located in the central part of Fig. 8a. It contained a nucleus in the centre with darker contrast that probably comprise of a heavier element. Around the nucleus there are several segments with a layer structure growing out form the nucleus in different directions. This should be compared to the textured structure of the grains at the surface (Figs 5a and 6a). A schematic drawing of the different BN structures is given in Fig. 9.

Both in the bulk (Fig. 1a) and close to the surface (Fig. 8a), small particles with more or less circular cross-section were seen. The EDS spectra taken on several of these revealed only Si. Some of them look like spherical inclusions in larger grains. This type of inclusions have been found by others [6]. One example, spherical grains attached to a larger grain (see Fig. 10a) was analysed

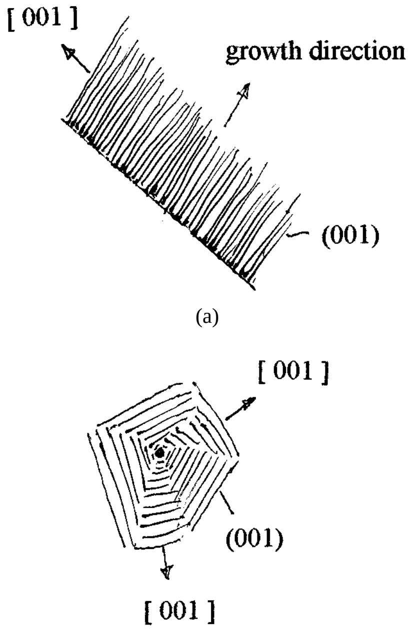

(a)

(b)

Figure 9 Schematic drawing of different hexagonal BN. (a) Textured BN, platelets are parallel to each other and perpendicular to their common [001] direction. The (001) planes grow unidirectionally; (b) BN around nucleus, the grain appears to grow radially from a central nucleus by forming racks of (001) planes.

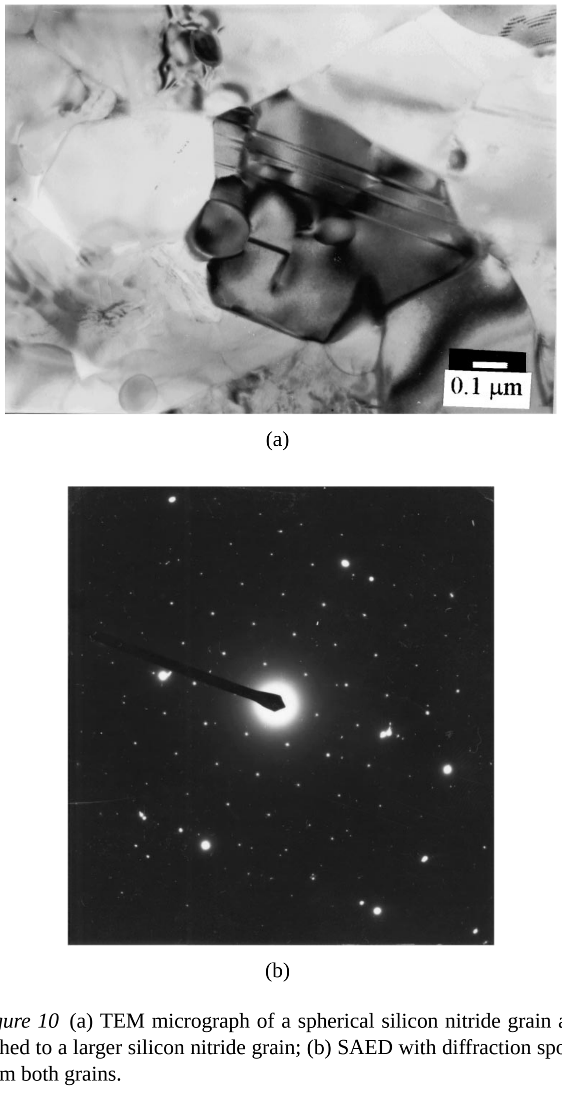

(a)

(b)

Figure 10 (a) TEM micrograph of a spherical silicon nitride grain attached to a larger silicon nitride grain; (b) SAED with diffraction spots from both grains.

further. A series of SAED patterns was taken from the small round particle. A low index pattern with a zone axis [001] is shown in Fig. 10b. Diffraction from the larger grain is also present. Both grains are β-Si_3N_4 but with different crystallographic orientations. A glassy phase surrounded the spherical particle.

4. Comments on BN formation and encapsulation glass penetration

When the pressure is applied during the HIP-cycle, the viscous encapsulation glass is pushed into the open pores of the ceramic green body. This is discussed in an earlier study [7]. If nothing were to hinder the viscous flow of the pure borosilicate glass, calculations applying Darcy's law predict that the encapsulation glass should penetrate hundreds to thousands of microns into the ceramic component, but such significant glass intrusion could not be experimentally observed. BN formation has been proposed as a possible mechanism for the prevention of penetration in borosilicate glass encapsulation [8, 9]. Modification of the glass composition during the HIP-cycle, for example, with nitrogen and silica dissolved in the glass and interaction between the glass and the pore walls are also processes which may hinder deep glass infiltration [7]. A full clarification of the mechanisms has not been obtained.

The boron nitride with the textured structure seems to nucleate heterogeneously on the surface grains. In Fig. 5a the colony of lamellae decreases in width inwards and could correspond to a former pore channel. If this type of boron nitride forms when the glass starts to penetrate the small pore channels of the green body then the glass flow would be hindered. The formation of BN in the Si_3N_4-SiO_2-B_2O_3 system is thermodynamically favourable already at the temperature for pressure application, approximately 1200 °C [9]. Thus, boron nitride formation could well be one of the main mechanisms that hinder glass penetration during the HIP-cycle.

In greater detail, the process for this might be as follows. The viscous glass is pushed towards the outer grains of the silicon nitride surface and into the open pore channels (mean diameter typically around 50 nm). Firstly, the thin silica layer (approximately 0.7 nm thick) on the silicon nitride grain surfaces will react with the glass and be dissolved. On the silicon nitride surfaces a heterogeneous nucleation takes place and a number of boron nitride crystals start to grow. They grow by extending the (001) planes outwards into the melted encapsulation glass. As soon as the formation of this BN starts, the flow of the glass will be hindered because the pore channels become narrower. When the crystals have grown to a certain length, or volume, the boron-containing glass loses direct contact with the silicon nitride. The growth process will slow down due to the longer diffusion paths for nitrogen. The boron nitride colonies are limited in size to approximately 0.5 microns, but this would be enough to prevent the glass from deep penetration into the ceramic material. The silicon nitride grains depleted in nitrogen form oxynitride.

The other type of hexagonal BN grains seem to form around a nucleus. The crystals have evidently been able to grow in different directions, as would be the case in a larger volume of glass melt. The glassy phases of silicon nitride materials are known to contain nitrogen [10] and oxynitride formation yields nitrogen as a product. During the HIP process nitrogen may diffuse out towards the encapsulation glass and together with the boron form BN around suitable nuclei, such as inhomogeneities in the glass, for example, small undissolved SiO_2 grains.

BN grains grown around a nucleus were also found further into the silicon nitride albeit close to the surface. For these to form, boron must be transported into the ceramic. In an earlier study of a similiar system with interrupted HIP-cycles, some boron were detected using SIMS (secondary ion mass spectroscopy) analysis [7]. Boron had diffused some hundreds of microns into the silicon nitride material already at 1200°C upon first pressure application. Since the diffusion is usually much faster in the glassy phase than in the crystals, this boron is presumably concentrated in the glassy phase of the material implying that BN would crystallise from this glass.

References

1. M. KNUTSON-WEDEL, L. K. L. FALK and T. EKSTRÖM, *Journal of Hard Materials* **3** (3/4) (1992) 435.
2. H. BJÖRKLUND, K. L. K. FALK, J. WASÉN, J. ADLERBORN and H. T. LARKER, in Materials Research Society Symposium Proceedings, V287 (1993) 423.
3. J. CHEN, J. SJÖBERG, O. LINDQVIST, C. O'MEARA and L. PEJRYD, *Journal of the European Ceramic Society* **7** (1991) 319.
4. A. BARNA, in Specimen Preparation for TEM of Materials III, Material Research Society Symposium Proceeding, V254, edited by R. Anderson, B. Tracy and J. Bravman (1992) p. 3.
5. A. K. WESTMAN, L. Y. WEI and F. BARRE, *Microscopy Research and Technique* **45**(3) (1999) 198.
6. K. L. K. FALK, G. L. DUNLOP and R. POMPE, *Materials Science and Engineering* **71** (1985) 123.
7. A.-K. WESTMAN and H. T. LARKER, *Journal of the European Ceramic Society* **19** (1999) 2739.
8. J. ADLERBORN, H. T. LARKER, B. MATTSSON and J. NILSSON, German Patent no. 2 950158, US Patent no. 4478789 (1978).
9. A.-K. WESTMAN, S. FORSBERG and H. T. LARKER, *Journal of the European Ceramic Society* **18** (1998) 633.
10. S. HAMPSHIRE, R. A. L. DREW and K. H. JACK, *Com. Am. Ceram. Soc.* **67** (1984) C45.

Received 25 August 1998
and accepted 19 November 1999